AERO. & ASTRO. LIBRARY

MASS. INST. TECH.
DEC 8 1945
LIBRARY

AERO

NATIONAL ADVISORY COMMITTEE FOR AERONAUTICS

REPORT No. 738

Copy 3

GROUND EFFECT ON DOWNWASH ANGLES AND WAKE LOCATION

By S. KATZOFF and HAROLD H. SWEBERG

1943

AERONAUTIC SYMBOLS

1. FUNDAMENTAL AND DERIVED UNITS

	Symbol	Metric		English	
		Unit	Abbreviation	Unit	Abbreviation
Length	l	meter	m	foot (or mile)	ft (or mi)
Time	t	second	s	second (or hour)	sec (or hr)
Force	F	weight of 1 kilogram	kg	weight of 1 pound	lb
Power	P	horsepower (metric)		horsepower	hp
Speed	V	kilometers per hour	kph	miles per hour	mph
		meters per second	mps	feet per second	fps

2. GENERAL SYMBOLS

W Weight $=mg$

g Standard acceleration of gravity $=9.80665$ m/s^2 or 32.1740 ft/sec^2

m Mass $=\frac{W}{g}$

I Moment of inertia $=mk^2$. (Indicate axis of radius of gyration k by proper subscript.)

μ Coefficient of viscosity

ν Kinematic viscosity

ρ Density (mass per unit volume)

Standard density of dry air, 0.12497 kg-m^{-4}-s^2 at 15° C and 760 mm; or 0.002378 lb-ft^{-4} sec^2

Specific weight of "standard" air, 1.2255 kg/m^3 or 0.07651 lb/cu ft

3. AERODYNAMIC SYMBOLS

S Area

S_w Area of wing

G Gap

b Span

c Chord

A Aspect ratio, $\frac{b^2}{S}$

V True air speed

q Dynamic pressure, $\frac{1}{2}\rho V^2$

L Lift, absolute coefficient $C_L=\frac{L}{qS}$

D Drag, absolute coefficient $C_D=\frac{D}{qS}$

D_0 Profile drag, absolute coefficient $C_{D_0}=\frac{D_0}{qS}$

D_i Induced drag, absolute coefficient $C_{D_i}=\frac{D_i}{qS}$

D_p Parasite drag, absolute coefficient $C_{D_p}=\frac{D_p}{qS}$

C Cross-wind force, absolute coefficient $C_C=\frac{C}{qS}$

i_w Angle of setting of wings (relative to thrust line)

i_t Angle of stabilizer setting (relative to thrust line)

Q Resultant moment

Ω Resultant angular velocity

R Reynolds number, $\rho\frac{Vl}{\mu}$ where l is a linear dimension (e.g., for an airfoil of 1.0 ft chord, 100 mph, standard pressure at 15° C, the corresponding Reynolds number is 935,400; or for an airfoil of 1.0 m chord, 100 mps, the corresponding Reynolds number is 6,865,000)

α Angle of attack

ϵ Angle of downwash

α_0 Angle of attack, infinite aspect ratio

α_i Angle of attack, induced

α_a Angle of attack, absolute (measured from zero-lift position)

γ Flight-path angle

REPORT No. 738

GROUND EFFECT ON DOWNWASH ANGLES AND WAKE LOCATION

By S. KATZOFF and HAROLD H. SWEBERG
Langley Memorial Aeronautical Laboratory
Langley Field, Va.

477390—43

NATIONAL ADVISORY COMMITTEE FOR AERONAUTICS

HEADQUARTERS, 1500 NEW HAMPSHIRE AVENUE NW., WASHINGTON, D. C.

Created by act of Congress approved March 3, 1915, for the supervision and direction of the scientific study of the problems of flight (U. S. Code, title 50, sec. 151). Its membership was increased to 15 by act approved March 2, 1929. The members are appointed by the President, and serve as such without compensation.

JEROME C. HUNSAKER, Sc. D., *Chairman*, Cambridge, Mass.

GEORGE J. MEAD, Sc. D., *Vice Chairman*, Washington, D. C.

CHARLES G. ABBOT, Sc. D., Secretary, Smithsonian Institution.

HENRY H. ARNOLD, Lieutenant General, United States Army, Commanding General, Army Air Forces, War Department.

LYMAN J. BRIGGS, Ph. D., Director, National Bureau of Standards.

W. A. M. BURDEN, Special Assistant to the Secretary of Commerce.

VANNEVAR BUSH, Sc. D., Director, Office Scientific Research and Development, Washington, D. C.

WILLIAM F. DURAND, Ph. D., Stanford University, Calif.

O. P. ECHOLS, Major General, United States Army, Commanding General, The Matériel Command, Army Air Forces, War Department.

SYDNEY M. KRAUS, Captain, United States Navy, Bureau of Aeronautics, Navy Department.

FRANCIS W. REICHELDERFER, Sc. D., Chief, United States Weather Bureau.

JOHN H. TOWERS, Rear Admiral, United States Navy, Chief, Bureau of Aeronautics, Navy Department.

EDWARD WARNER, Sc. D., Civil Aeronautics Board, Washington, D. C.

ORVILLE WRIGHT, Sc. D., Dayton, Ohio.

THEODORE P. WRIGHT, Sc. D., Assistant Chief, Aircraft Branch, War Production Board.

GEORGE W. LEWIS, *Director of Aeronautical Research*

JOHN F. VICTORY, *Secretary*

HENRY J. E. REID, *Engineer-in-Charge, Langley Memorial Aeronautical Laboratory, Langley Field, Va.*

SMITH J. DEFRANCE, *Engineer-in-Charge, Ames Aeronautical Laboratory, Moffett Field, Calif.*

EDWARD R. SHARP, *Administrative Officer, Aircraft Engine Research Laboratory, Cleveland Airport, Cleveland, Ohio*

TECHNICAL COMMITTEES

AERODYNAMICS
POWER PLANTS FOR AIRCRAFT
AIRCRAFT MATERIALS
AIRCRAFT STRUCTURES
INVENTIONS & DESIGNS
OPERATING PROBLEMS

Coordination of Research Needs of Military and Civil Aviation

Preparation of Research Programs

Allocation of Problems

Prevention of Duplication

Consideration of Inventions

LANGLEY MEMORIAL AERONAUTICAL LABORATORY
LANGLEY FIELD, VA.

AMES AERONAUTICAL LABORATORY
MOFFETT FIELD, CALIF.

AIRCRAFT ENGINE RESEARCH LABORATORY
CLEVELAND AIRPORT, CLEVELAND, OHIO

Conduct, under unified control, for all agencies, of scientific research on the fundamental problems of flight.

OFFICE OF AERONAUTICAL INTELLIGENCE
WASHINGTON, D. C.

Collection, classification, compilation, and dissemination of scientific and technical information on aeronautics

REPORT No. 738

GROUND EFFECT ON DOWNWASH ANGLES AND WAKE LOCATION

By S. Katzoff and Harold H. Sweberg

SUMMARY

A theoretical study has been made of the reduction in downwash and the upward displacement of the wake in the presence of the ground, and some verification of the theory has been obtained by means of air-flow measurements made with a ground-board and image-wing combination. Methods are given for estimating the effects and numerous examples are included to illustrate the nature of these effects and to show their order of magnitude.

INTRODUCTION

An important consideration in the analysis of the handling characteristics of an airplane is the large reduction of downwash in take-off or in landing occasioned by the proximity of the ground. A related consideration is that the wing wake, which under normal flight conditions generally passes below the tail, is displaced upward by the ground and may envelop the tail just as a landing is about to be made.

The basis for the calculation of downwash angles and wake characteristics for the normal condition (without ground effect) is discussed at length in reference 1; a résumé of the theory is given in reference 2, together with numerous charts to facilitate its application. The present paper is essentially a supplement to these papers and extends the theory and the methods of calculation to cover take-off or landing conditions. It includes also a sufficient number of illustrative examples to enable the designer to estimate the effects of the ground on the wake location and on the downwash angles.

A few wind-tunnel tests were made to provide some verification of the theory and to indicate that no important factors had been neglected.

SYMBOLS

C_L	lift coefficient
C_{L_w}	lift coefficient at a particular angle of attack, flaps up
C_{L_f}	increase of lift coefficient, at same angle of attack, on deflecting the flap
c_{d_0}	section profile-drag coefficient
A	aspect ratio
α	angle of attack
ϵ	downwash angle
ϵ_w	downwash angle contributed by plain wing
ϵ_f	downwash angle contributed by flap
b	span
c	chord
c_r	root chord
$\bar{c}$	mean aerodynamic chord
z	vertical distance from ground to wake origin at root section
d	distance from wing aerodynamic center to ground
h	downward displacement of center line of wake from its origin at trailing edge, measured normal to relative wind
m	vertical distance from elevator hinge axis to wake origin at root section, measured normal to relative wind (positive if hinge axis is above trailing edge)
x	longitudinal distance from elevator hinge axis to quarter-chord point of root section
ξ	longitudinal distance from elevator hinge axis to trailing edge of root section
ζ	wake half-width
σ	correction factor in formula for ground effect on angle of attack
q	free-stream dynamic pressure

THEORY

In the proximity of the ground, the wing vortex system is reflected in the ground and the resulting downwash at the tail corresponds to the combined field of flow of the two symmetrically situated and oppositely rotating vortex systems. The superposition is illustrated in figure 1. Figure 1(a) shows the downwash field in the plane of symmetry of a wing, under normal flight conditions; the field is symmetrical about the wake, which is so curved that its slope at every point is the tangent of the downwash angle at that point. The superposition of the reflected downwash field when the wing is near the ground is shown in figure 1 (b); the downwash angle at every point is the algebraic sum of the two downwash angles, and the slope of the wake at every point is the tangent of the resultant downwash angle at that point. The resultant field is shown in figure 1(c).

Aero 7 Dec. '45

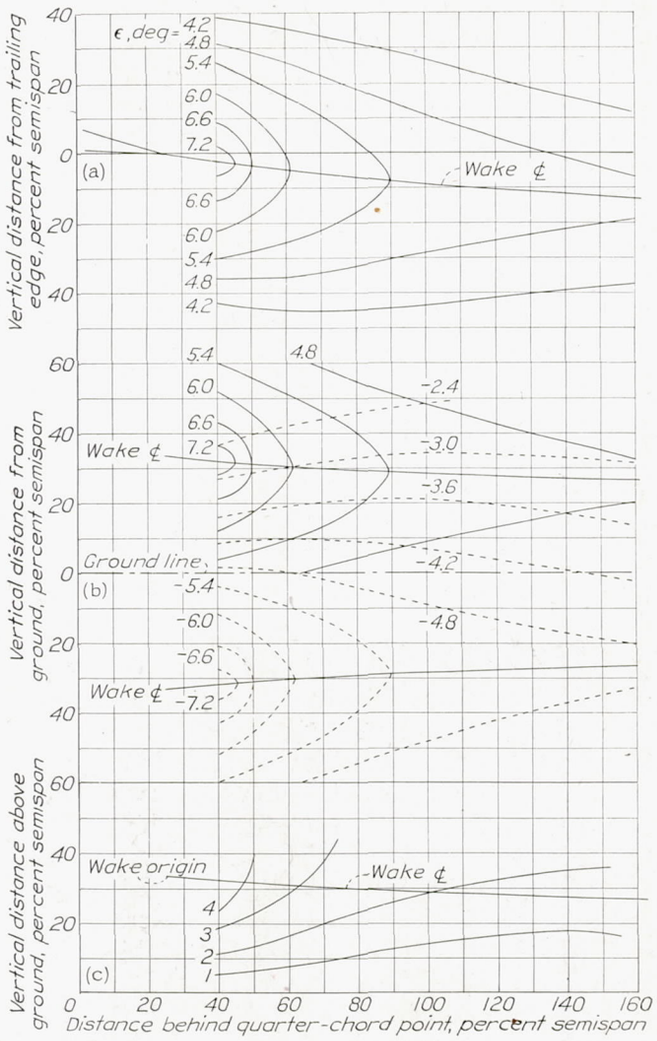

(a) Normal downwash field.
(b) Superposition of downwash fields of actual vortex system (full lines) and reflected vortex system (dotted lines).
(c) Resultant downwash field.

FIGURE 1.—Illustration of the ground effect on the downwash field behind an airfoil. Rectangular wing; A, 6; C_L, 1.0; $z/\bar{c}$, 1.0.

The assumption, implied in this procedure, that the system of bound and trailing vortices is independent of the distance from the ground does not strictly hold. First, since the field of the reflected bound vortex reduces the effective airspeed at the wing, the average strength of the bound vortex must be correspondingly increased in order to maintain the given lift coefficient. This increase is about $\frac{3.5C_L}{d/\bar{c}}$ percent, and the results obtained by the procedure given may, for better accuracy, be increased by this amount. Second, the distribution of the bound vortex across the span of the wing will be altered by the presence of the ground with, usually, a slight concentration toward the center of the wing. Third, the trailing vortices shed from the tips of the wings and the flaps do not extend straight back but move laterally outward under the influence of their own reflections. The last two effects are relatively

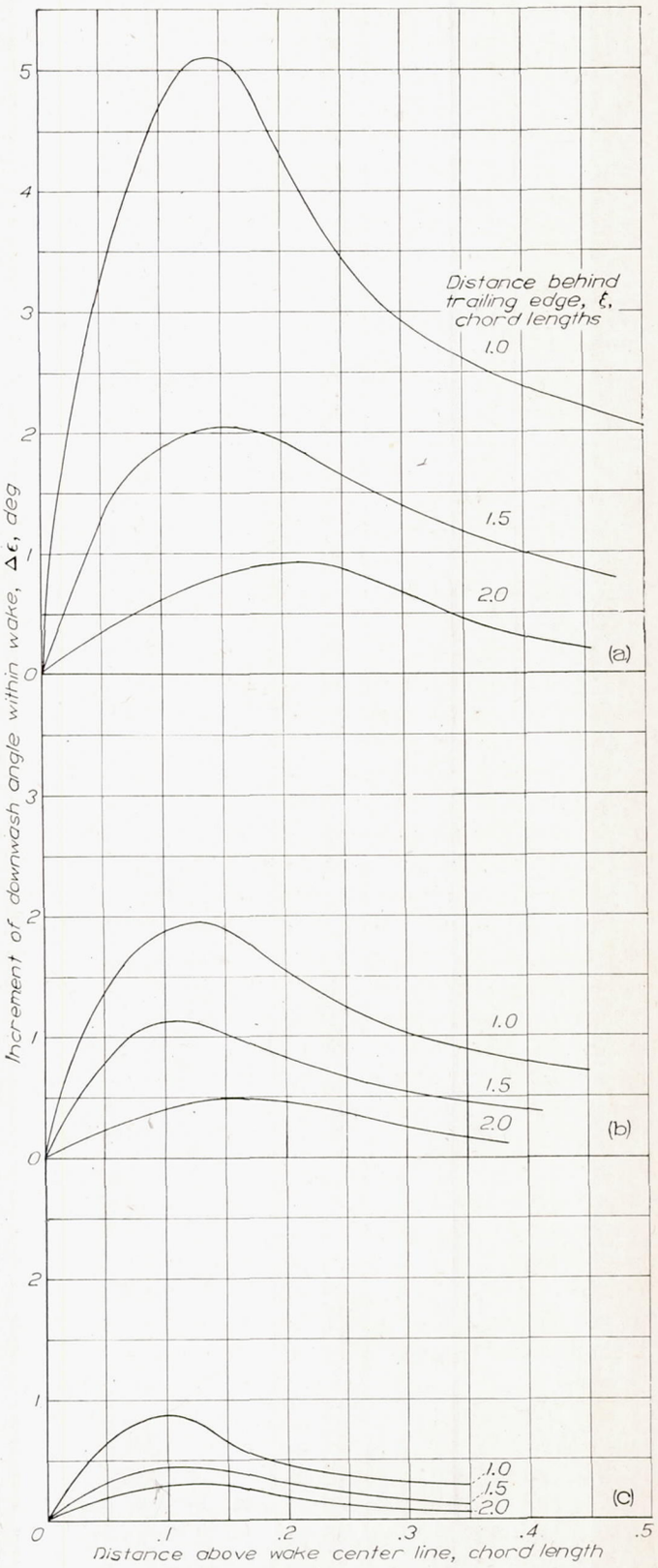

(a) $c_{d_0}=0.20$.
(b) $c_{d_0}=0.15$.
(c) $c_{d_0}=0.10$.

FIGURE 2.—Wake effect on downwash. The effects are equal but of opposite sign below the wake center.

small and are probably negligible for most cases. For a practical first approximation it appears permissible to neglect all three effects because, for distances from the ground for which they become pronounced, the downwash angles are so far reduced that even relatively large percentage errors are numerically small.

The wake, together with the flow into it (reference 2), may also be considered to be reflected in the ground. Inasmuch as this inflow is appreciable only within or very close to the wake, the effect of the reflected wake will generally be negligible unless the wing is less than one chord from the ground.

The analysis given in reference 2 of the flow into the wake has been repeated on the basis of the more recent wake studies included in reference 3. The results (fig. 2) indicate that the effect is less than that shown in reference 2, especially near the edge of the wake.

It may be remarked here, with respect to the actual prediction of tail forces, that some uncertainty exists regarding the calculation of the effective angle of attack of the tail when it is near the center of the wake, where the wake effect changes rapidly with distance from the center. For such conditions, the relation between the effective flow at the tail and the flow which would exist in that region in the absence of the tail may not be very close. Experimental studies of the forces on an airfoil in a nonhomogeneous field of flow, as in a wake, would be of considerable aid in this respect.

It may be noted further that the methods of reference 2 are not very accurate in certain cases, for example, if the fuselage is a poor aerodynamic body or if the additional lift due to flap deflection does not carry across the fuselage. Such inaccuracy may be expected to persist near the ground; prediction of the wake location, which will often be the most critical of the variables involved, will be relatively unaffected by these inaccuracies.

APPARATUS AND TESTS

For the tests the ground was represented, as suggested in reference 4, by an image airfoil and a ground board having its leading edge midway between the test airfoil and the image (indicated diagrammatically in fig. 3). The test airfoil was a 10- by 60-inch rectangular NACA CYH airfoil equipped with pressure orifices along the mid-semispan section; the image airfoil was similar in form but had a Clark Y section. No balance was used; the relation between the lift coefficient at the section containing the orifices and the lift coefficient of the wing, as determined from previous tests, was used to estimate the lift. The ground board was of ¾-inch plywood; although probably too thick for the usual studies of ground effect on lift and drag, it was considered satisfactory for downwash studies. The airfoils and the ground board were mounted vertically on the floor of the entrance cone of the NACA full-scale wind tunnel (fig. 4); the alinement of the ground board with the air stream was verified by means of static-pressure measurements made near the leading edge on both sides. Airspeeds of about 50 miles per hour were used for the tests.

FIGURE 3.—Partial ground board and image-wing combination.

Measurements of downwash angles and of total and static pressures were made in the plane of symmetry of the airfoil by means of a two-finger yaw head (reference 5) and a total-pressure tube and a static-pressure tube placed near it (fig. 4). One test was made of the plain

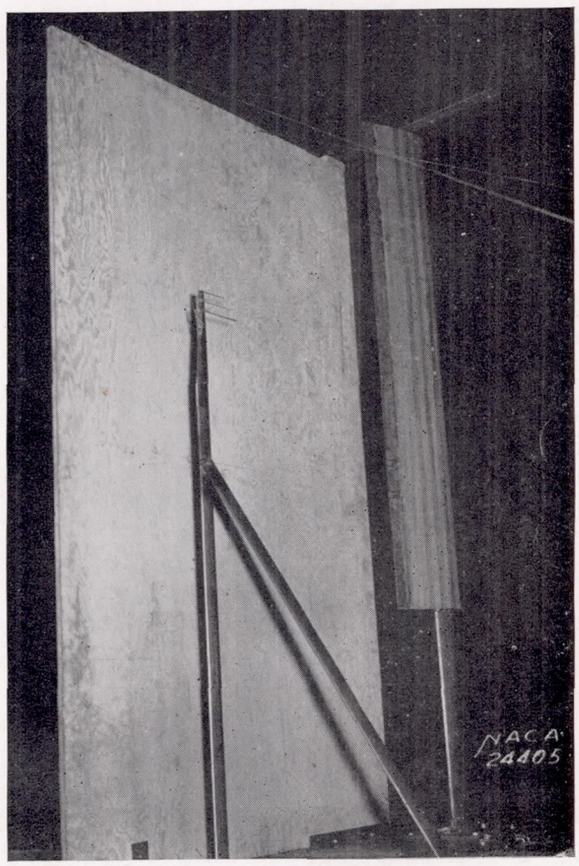

FIGURE 4.—Set-up for measuring ground effect on downwash.

airfoil at a distance of 1.0c (measured to the quarter-chord line) from the ground, at a lift coefficient of 1.0. For the airfoils fitted with full-span 0.20c split flaps deflected 60°, measurements were made at distances of 0.6c, 1.0c, and 1.4c from the ground at a lift coefficient of about 1.6.

The accuracy with which the airfoil lift coefficients were estimated from the section lift coefficients was considered satisfactory, although the relation between the two is probably altered somewhat in the presence of the ground. Most of the downwash angles are accurate within about 0.25°. In the wake, however, especially near the trailing edge, the excessive turbulence probably contributed further error, as was indicated by the fact that the separate pressure readings of the two fingers of the yaw head did not bear the same relation to their difference as did the readings outside the wake.

The combination of the partial ground board and an image wing is probably the most practical of the acceptable methods of studying ground effect on airfoils. As has been shown by a number of investigators, the boundary layer on a ground board that extends ahead of the airfoil expands or separates as it approaches the area under the leading edge of the airfoil, owing to the positive pressure gradient in that region. For the combination, however, the leading edge of the board is at the region of maximum pressure and the boundary layer develops in a negative pressure gradient. Some preliminary studies indicated that this negative gradient continues for some distance behind the airfoil and that the boundary layer remains of negligible thickness throughout the region where it might influence the airfoil characteristics. Apparently, the image wing need not be an exact reproduction of the test wing (reference 4); the thickness of the leading edge of the ground board should be reasonably small, however, for the leading edge corresponds essentially to a discontinuity in the ground level.

RESULTS OF TESTS AND DISCUSSION

The experimental downwash-angle contours are compared with the calculated contours in figure 5. Since the observed wake of the flapped airfoil indicated a profile-drag coefficient of about 0.135, the wake effect corresponding to this value was included in the calculated contours.

The main discrepancy between the experimental and the calculated values of ϵ appears in the region close to the trailing edge, where the experimental values are higher than the theoretical; a vortex at the quarter-chord line is apparently too inexact a substitute for a wing, especially a flapped wing, to give accurate results for the flow near it. In the region where the tail surface is usually placed, however, the agreement is satisfactory. The observed variation in downwash across the wake seemed to be somewhat less sharp than that indicated by the theory; as has already been noted, however, the measurements within the wake were relatively inaccurate. Inasmuch as the calculated and the observed locations of the wake center line agreed within the accuracy of the measurements, only one wake center line is shown in each figure.

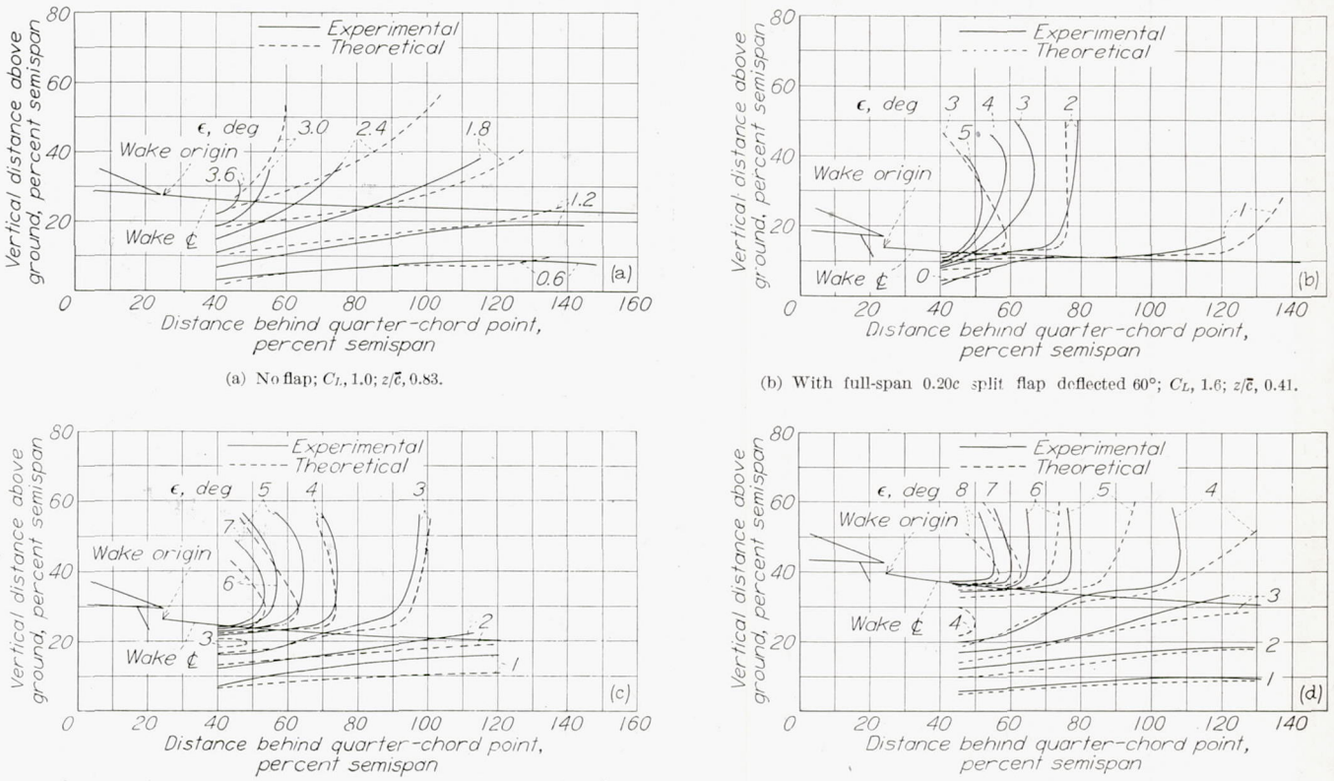

(a) No flap; C_L, 1.0; $z/\bar{c}$, 0.83.

(b) With full-span 0.20c split flap deflected 60°; C_L, 1.6; $z/\bar{c}$, 0.41.

(c) With full-span 0.20c split flap deflected 60°; C_L, 1.6; $z/\bar{c}$, 0.78.

(d) With full-span 0.20c split flap deflected 60°; C_L, 1.6; $z/\bar{c}$, 1.18.

FIGURE 5.—Comparison of theoretical with experimental downwash angles in the presence of the ground. Rectangular NACA CYH wing. A, 6.

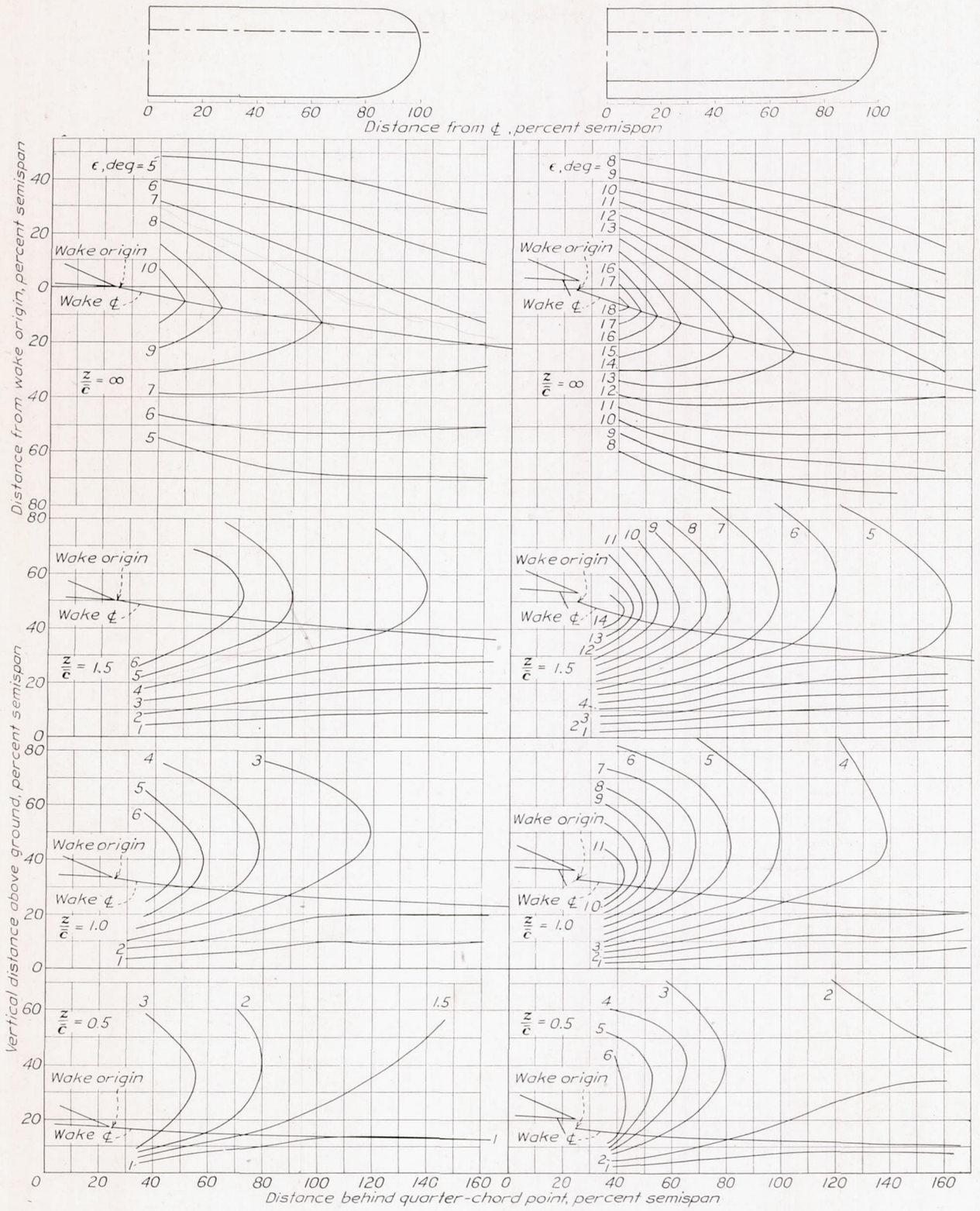

Plain wing; C_L, 1.5 Full-span flap; C_L, 2.5

FIGURE 6.—Theoretical downwash-angle contours and wake positions for various distances from ground. A, 6; taper ratio, 1:1.

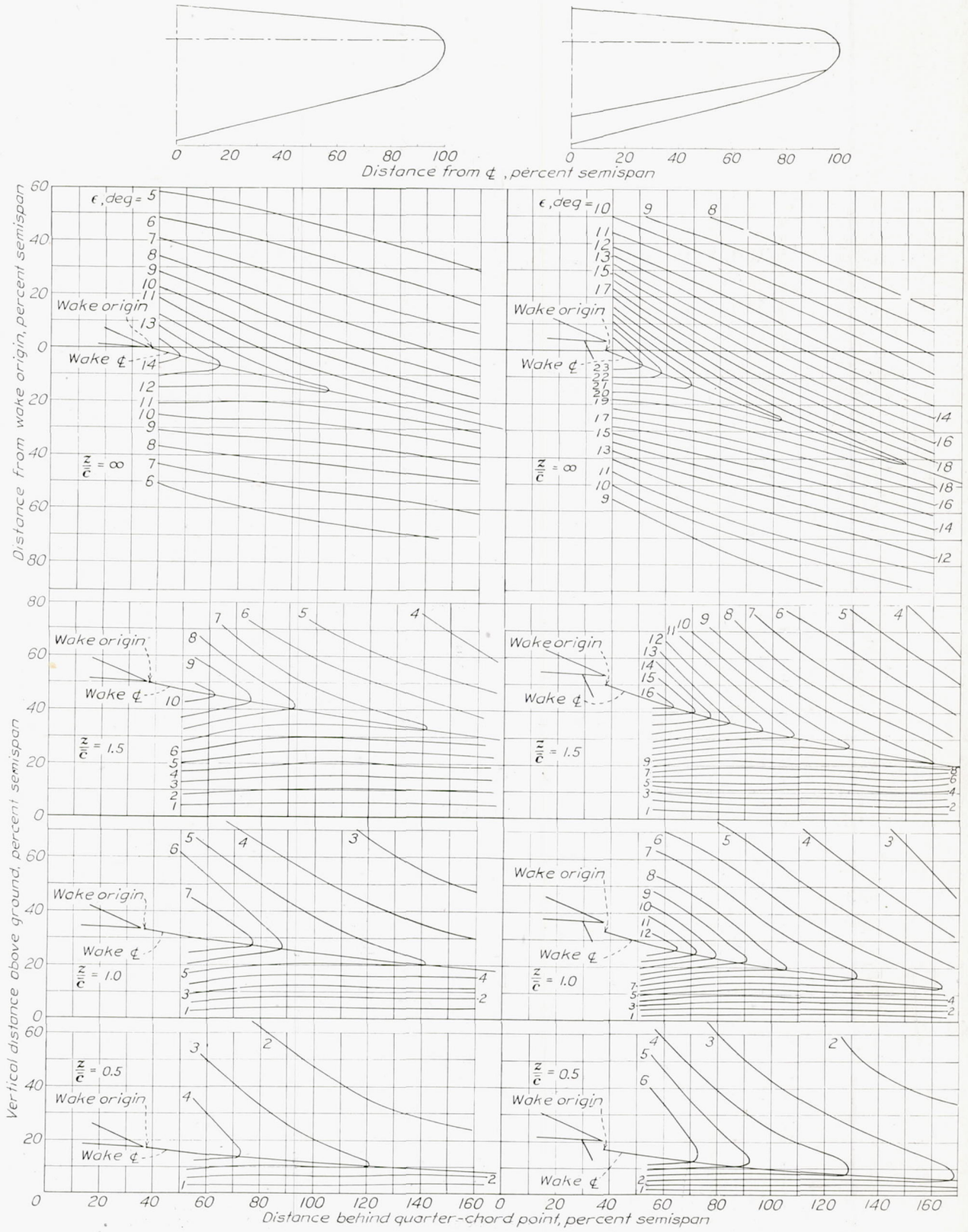

Plain wing; C_L, 1.5 Full-span flap; C_L, 2.5

FIGURE 7.—Theoretical downwash-angle contours and wake positions for various distances from ground. A, 6; taper ratio, 3:1.

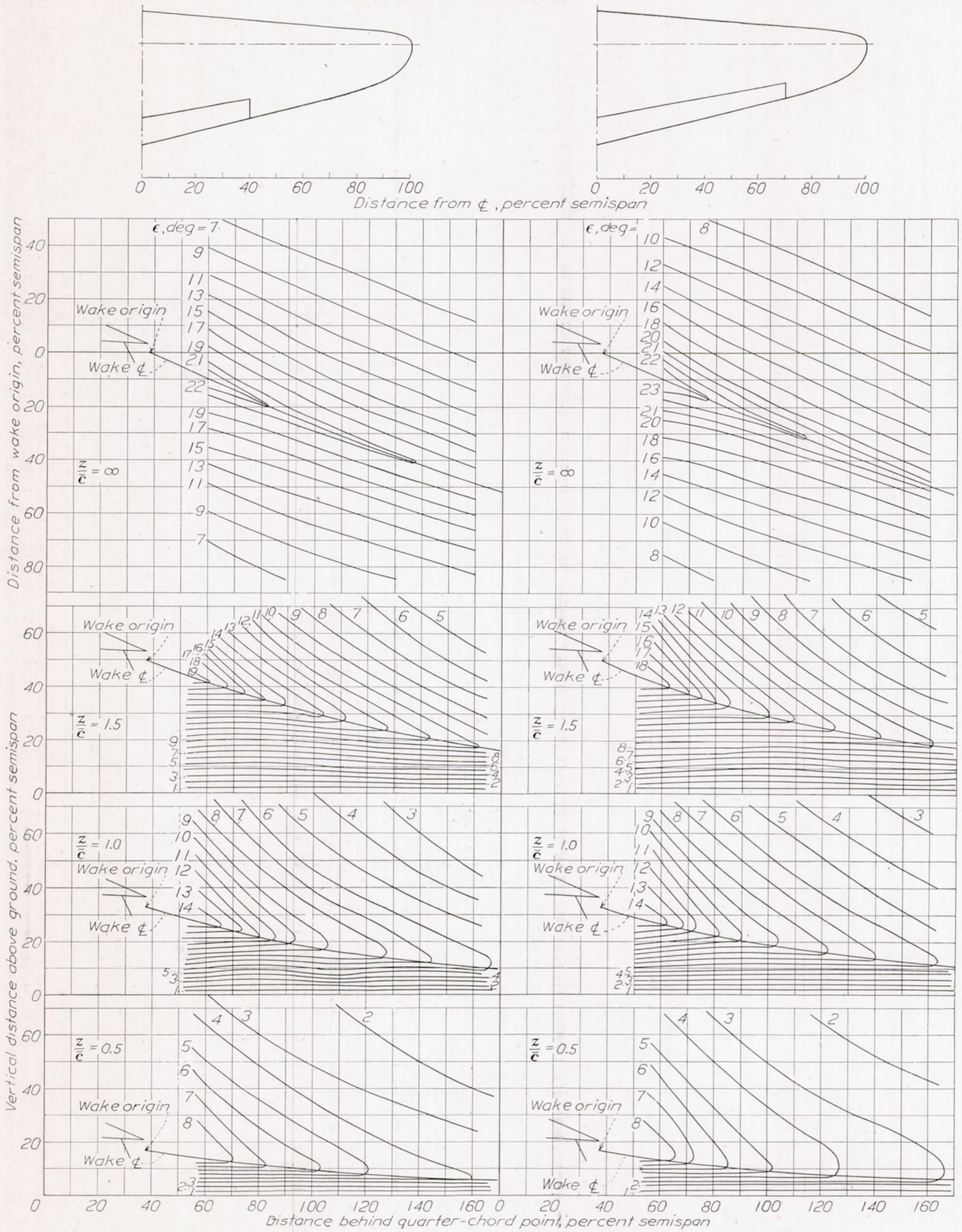

0.4-span flap; C_{L_w}, 1.2; C_{L_f}, 0.6 — 0.7 span flap; C_{L_w}, 1.2; C_{L_f}, 1.2

FIGURE 8.—Theoretical downwash-angle contours and wake positions for various distances from ground. A, 6; taper ratio, 3:1.

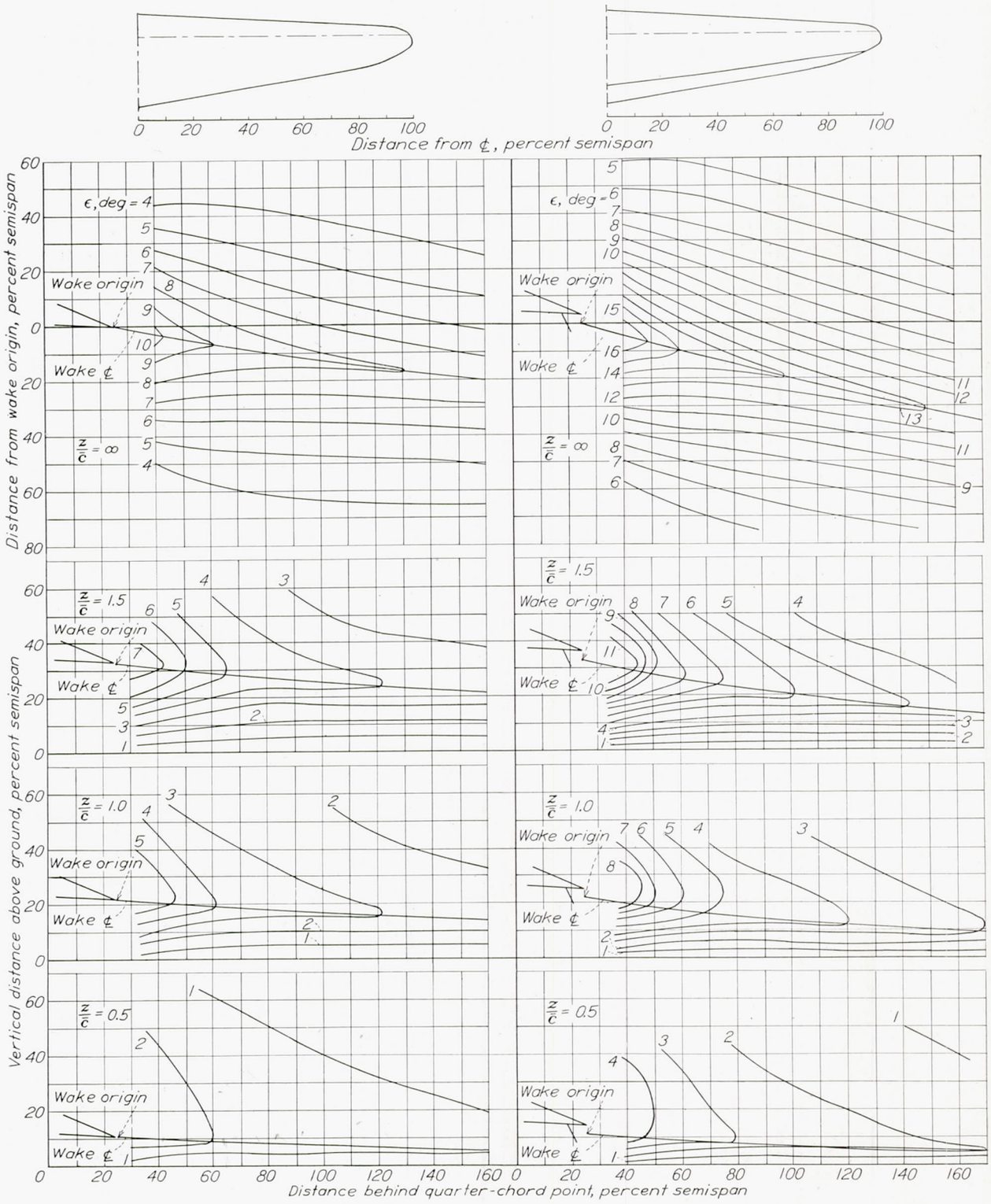

Plain wing; C_L, 1.5 Full-span flap; C_L, 2.5

FIGURE 9.—Theoretical downwash-angle contours and wake positions for various distances from ground. A, 9; taper ratio, 3:1.

APPLICATION

EXAMPLES OF GROUND EFFECT

A number of examples of the ground effect on downwash angles and wake location are given in figures 6 to 10. These figures may be used for design charts because the examples cover most conditions of practical interest; that is, enough cases are included not only to illustrate the nature of the effect but also to permit an estimate of the order of magnitude of the effect in any case. For use at lift coefficients other than those shown, the downwash angles and the downward displacement of the wake may be assumed proportional to the lift coefficient. No wake effect was included in the computations for these figures inasmuch as the profile-drag coefficient would depend on the type of high-lift device used; the correction for the ground effect on the effective airspeed at the wing has also been omitted because the value of $d/\bar{c}$ depends to some extent on the geometric characteristics of the wing.

CALCULATION PROCEDURE

Figures 6 to 10, together with figure 2, will probably suffice to indicate to the designer the magnitude of the ground effect and the conditions that the airplane must meet near the ground. In order to complete the presentation and also to show the methods of calculation for cases not covered by the illustrations, the following additional discussion of the method is given.

Superposition of the downwash fields.—The only complication of the process of superposition illustrated in figure 1 is that the location of the wake cannot be predetermined because it depends on the resultant downwash field. For any particular case, a satisfactory method of locating the wake is to assume a wake location, calculate the corresponding downwash angles along it, adjust the wake location to these angles, recalculate the downwash angles, readjust the wake location, and so on until further steps produce no change. Two or three steps generally suffice.

Another method is to draw the wake center line as a series of straight sections starting at the trailing edge (or wake origin), the slope of each section being determined by the coordinates of its first point. (This method corresponds to the step-by-step integration of the differential equation, $dy/dx=f(x, y)$.) A modification of this method was found to be simplest for locating the wake at any particular distance behind the trailing edge within the normal range of tail positions. It depends on the observation that, in this range, the average slope of the wake between the trailing edge and a point distant ξ behind it is very nearly the slope of the wake at 0.45ξ from the trailing edge, while the average slope between the trailing edge and the point at 0.45ξ is very nearly the slope at 0.20ξ from the trailing edge. These relations are illustrated in figure 11. The method

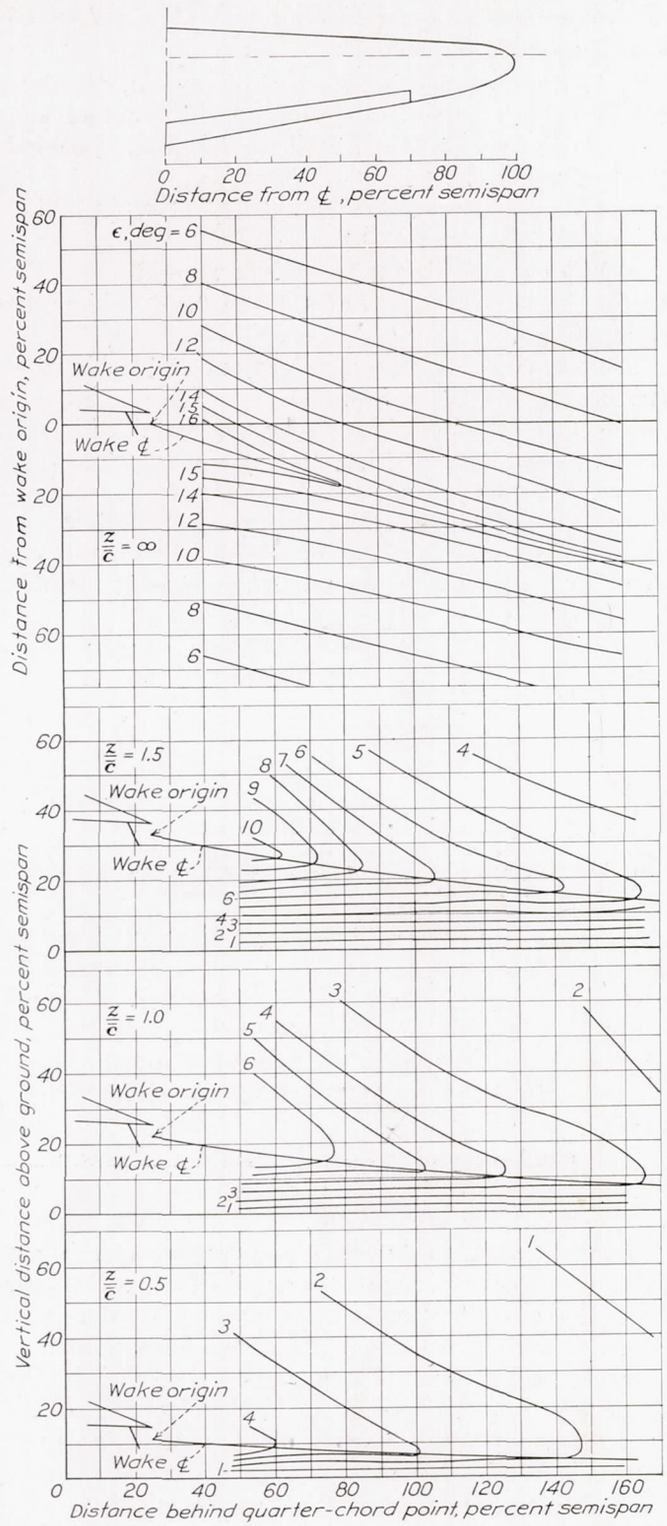

FIGURE 10.—Theoretical downwash-angle contours and wake positions for various distances from ground. A, 9; taper ratio, 3:1. 0.7-span flap; C_{L_w}, 1.2; C_{L_f}, 1.2.

of computing the wake displacement at a distance ξ thus consists of the following steps:

a. Without considering wake displacement, calculate the downwash angle $\epsilon_{0.20}$ (resultant of the actual and the reflected vortex fields) in the wake at 0.20ξ behind the trailing edge.

b. Calculate the wake displacement at 0.45ξ behind the trailing edge as $0.45\xi \times \tan \epsilon_{0.20}$.

c. Taking this displacement into account, find the downwash angle $\epsilon_{0.45}$ in the wake at 0.45ξ behind the trailing edge.

d. Calculate the wake displacement at ξ behind the trailing edge as $\xi \times \tan \epsilon_{0.45}$.

The wake effect (fig. 2) is added as described in reference 2 with consideration, also, of the reflected wake for positions very close to the ground. For such positions it may happen that the wake half-width, as calculated by the methods of reference 2, exceeds the distance from the wake center to the ground. In this

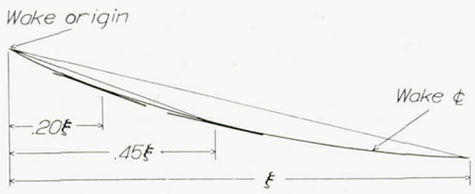

FIGURE 11.—Illustration of the simplified method of determining the wake displacement at a distance ξ behind the trailing edge. The average slope between the trailing edge and ξ approximately equals the slope at 0.45ξ and the average slope between the trailing edge and 0.45ξ approximately equals the slope at 0.20ξ.

case the ground effect will no longer be simply a reflection of the normal wake; for the calculation of downwash angles, however, the assumption of simple reflection will give approximately correct results though, physically, the corresponding concept of a wake image partly extending above the ground is obviously incorrect.

The small correction for the variation of downwash across the tail span (fig. 21 of reference 2) may be disregarded in these calculations.

Ground effect on lift.—Although this paper is not primarily concerned with the ground effect on the wing lift, some remarks concerning it may be in order, inasmuch as its magnitude must be known for any application of these results. For a given lift coefficient, the angle of attack decreases as the airplane approaches the ground; hence the corresponding increase in the angle of attack of the tail is, for a given lift coefficient, less than the decrease in the angle of downwash.

The ground effect on the wing may be considered to consist essentially of three parts: (a) A reduction in the effective airspeed at the wing, due to the field of the reflected bound vortex; (b) a change in the effective camber and airfoil section characteristics in general, due to the curvature and the distortion of the flow by the reflected wing; and (c) a reduction in the induced angle at the wing, due to the upflow associated with the reflected trailing vortices. An extensive theoretical analysis is given in references 6 and 7, and the results are summarized in the appendix of reference 8. As indicated in reference 8, however, (c) alone appears to account approximately for the observed ground effect on lift, so that (a) and (b) may be considered to nullify each other for most conditions of practical interest. A simplified theory based on (c) alone may therefore be tentatively recommended, at least for stability and control calculations. The reduction in the angle of attack for a given lift coefficient is then given by the equation

$$\Delta\alpha = -57.3 \frac{C_L}{\pi A} \sigma$$

in which, by reference 8,

$$\sigma = e^{-2.48(2d/b)^{0.768}}$$

For the landing attitude, σ may be of the order of 0.5, which corresponds to the effective doubling of the aspect ratio.

RÉSUMÉ OF METHOD

For the calculation of downwash angles and wake location in the proximity of the ground, the procedure given in reference 2 is revised as follows:

Plain wings.—

1. Determine x, ξ, m, and z in semispans. (Consider the wake origin to coincide with the trailing edge.)

2. Determine the downward displacement h of the wake center line at the elevator position in the following steps:

a. Determine $\epsilon_{0.20}$ from the downwash charts of reference 2.

$$\epsilon_{0.20} = C_L[\epsilon(x-0.8\xi, 0) - \epsilon(x-0.8\xi, 2z)]$$

(The term $\epsilon(x-0.8\xi, 0)$ is the downwash angle read from the appropriate chart of reference 2 at the point whose abscissa is $x-0.8\xi$ and whose ordinate is 0. Similarly, the term $\epsilon(x-0.8\xi, 2z)$ is read at the point whose abscissa is $x-0.8\xi$ and whose ordinate is $2z$. It will be noted that the ordinates in the charts are thus considered as "vertical distances from the wake center"; the present label, "vertical distance from quarter-chord point," which applies only to the "undisplaced" downwash-angle contours, has given rise to some confusion.)

b. Determine $\epsilon_{0.45}$ from the downwash charts.

$$\epsilon_{0.45} = C_L\{\epsilon(x-0.55\xi, 0) - \epsilon[x-0.55\xi, 2(z-0.45\xi \tan \epsilon_{0.20})]\}$$

c. $h = \xi \tan \epsilon_{0.45}$

3. Determine the downwash at the hinge line as

$$\epsilon = C_L[\epsilon(x, m+h) - \epsilon(x, 2z+m-h)]$$

Flapped wings.—

1. Determine x, ξ, m, and z as before, but measure m and z from the wake origin rather than from the trailing edge.

2. Determine h in the following steps:

a. $$\epsilon_{0.20}=C_{L_w}[\epsilon_w x-.80\xi,\ 0)-\epsilon_w(x-0.8\xi,\ 2z)]$$
$$+C_{L_f}[\epsilon_f(x-0.8\xi,\ 0)-\epsilon_f(x-0.8\xi,\ 2z)]$$

where the subscripts of ϵ_w and ϵ_f signify that these values are to be read from the downwash charts for the plain wing and for the flap, respectively.

b. $$\epsilon_{0.45}=C_{L_w}\{\epsilon_w(x-0.55\xi,\ 0)-\epsilon_w[x-0.55\xi,\ 2(z-0.45\xi\tan\epsilon_{0.20})]\}$$
$$+C_{L_f}\{\epsilon_f(x-0.55\xi)-\epsilon_f[x-0.55\xi,\ 2(z-0.45\xi\tan\epsilon_{0.20})]\}$$

c. $$h=\xi\tan\epsilon_{0.45}$$

3. $$\epsilon=C_{L_w}[\epsilon_w(x,\ m+h)-\epsilon_w x,\ 2(z+m-h)]$$
$$+C_{L_f}[\epsilon_f(x,\ m+h)-\epsilon_f(x,\ 2z+m-h)]$$

4. Add the wake correction (fig. 2). This correction is a function of c_{d_0}, ξ (measured in root-chord lengths), and $m+h$ (measured in root-chord lengths).

5. Add the correction for the reflected wake, which is a function of c_{d_0}, ξ, and $2z+m-h$.

EXAMPLES

The specimen calculations of reference 2 will be repeated here for the case in which the trailing edge or wake origin is 0.2 semispan from the ground (fig. 12).

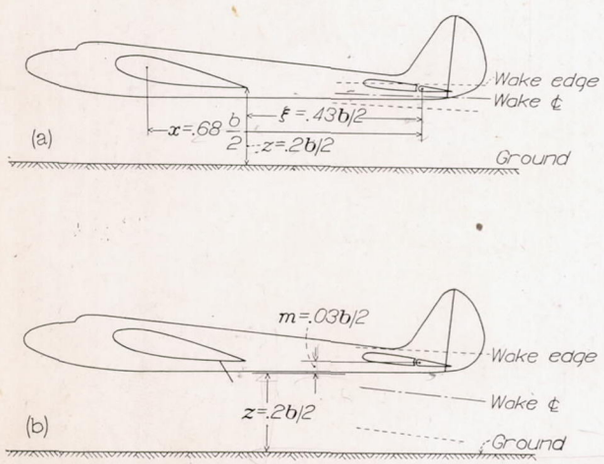

(a) Flap up.
(b) Flap down.

FIGURE 12.—Illustration for the specimen calculations of downwash and wake.

For the flap-up condition, the reduction in angle of attack for the given lift coefficient is about 0.7°; for the flap-down condition, the reduction is about 1.2°. These changes correspond to an increase in m of about $0.01b/2$. The steps just outlined are:

Flaps up.—

1. $x=0.68$, $\xi=0.43$, $m=0$, $z=0.2$

2. a. $$\epsilon_{0.20}=0.9[\epsilon(0.34,\ 0)-\epsilon(0.34,\ 0.4)]$$
$$=0.9\ (7.5°-3.2°)$$
$$=3.9°$$

(An extrapolation of the downwash-angle charts was necessary to find these values of ϵ.)

b. $$\epsilon_{0.45}=0.9[\epsilon(0.44,\ 0)-\epsilon(0.44,\ 0.37)]$$
$$=0.9(6.6°-3.5°)=2.8°$$

c. $$h=0.43\tan 2.8°$$
$$=0.02$$

3. $$\epsilon=0.9[\epsilon(0.68,\ 0.02)-\epsilon(0.68,\ 0.38)]$$
$$=0.9(5.8°-3.3°)$$
$$=2.3°$$

The wake half-width is about 0.03 semispan and the tail lies in it at 0.02 semispan from its center.

Flaps down.—

1. $x=0.68$, $\xi=0.43$, $m=0.03$, $z=0.2$

2. a. $$\epsilon_{0.20}=0.9[\epsilon_w(0.34,\ 0)-\epsilon_w(0.34,\ 0.4)]$$
$$+0.76[\epsilon_f(0.34,\ 0)-\epsilon_f(0.34,\ 0.4)]$$
$$=0.9(7.5°-3.2°)+0.76(9.5°-4.1°)$$
$$=3.9°+4.1°$$
$$=8.0°$$

b. $$\epsilon_{0.45}=0.9[\epsilon_w(0.44,\ 0)-\epsilon_w(0.44,\ 0.35)]$$
$$+0.76[\epsilon_f(0.44,\ 0)-\epsilon_f(0.44,\ 0.35)]$$
$$=0.9(6.6°-3.6°)+0.76(9.0°-4.6°)$$
$$=2.7°+3.3°$$
$$=6.0°$$

c. $$h=0.43\tan 6°$$
$$=0.05$$

3. $$\epsilon=0.9[\epsilon_w(0.68,\ 0.08)-\epsilon_w(0.68,\ 0.38)]$$
$$+0.76[\epsilon_f(0.68,\ 0.08)-\epsilon_f(0.68,\ 0.38)]$$
$$=0.9(5.3°-3.3°)+0.76(7.3°-4.2°)$$
$$=1.8°+2.4°$$
$$=4.2°$$

4. $$m+h=0.08 \text{ semispan}$$
$$=0.24c_r$$

Since the wake half-width ζ is $0.34c_r$, the tail is within the wake. Figure 2 indicates a downwash-angle increment of 1.5°.

5. $$2z+m-h=0.37 \text{ semispan}$$
$$=1.11c_r$$

The reflected wake is thus too far away to have an appreciable effect.

The downwash angle at the hinge line is

$$4.2°+1.5°=5.7°$$

which is 5° less than the value (10.7°) calculated for the case without ground effect. Since the attitude of the airplane has changed by 1.2°, the increase in the angle of attack of the tail is only 5°−1.2°, or 3.8°.

The dynamic pressure at the hinge line, $\frac{0.24}{0.34}=0.71$ wake half-width from the wake center, is (by fig. 24 of reference 2)

$$(1-0.2\times 0.63)q=0.87q$$

Langley Memorial Aeronautical Laboratory,
National Advisory Committee for Aeronautics,
Langley Field, Va., *October 3, 1941.*

REFERENCES

1. Silverstein, Abe, Katzoff, S., and Bullivant, W. Kenneth: Downwash and Wake behind Plain and Flapped Airfoils. Rep. No. 651, NACA, 1939.
2. Silverstein, Abe, and Katzoff, S.: Design Charts for Predicting Downwash Angles and Wake Characteristics behind Plain and Flapped Wings. Rep. No. 648, NACA, 1939.
3. Silverstein, Abe, and Katzoff, S.: A Simplified Method for Determining Wing Profile Drag in Flight. Jour. Aero. Sci., vol. 7, no. 7, May 1940, pp. 295–301.
4. Viaud, Louis: Méthode expérimentale pour l'étude en soufflerie de l'interaction au sol. Comptes Rendus, t. 206, no. 11, 14 March 1938, pp. 817–819.
5. Muttray, H.: Erfahrungen mit dem "Zweifinger-Abwindmessgerät" bei Strömungsrichtungsmessungen. Luftfahrtforschung, Bd. 15, Lfg. 3, 20. March 1938, pp. 123–124.
6. Tani, Itiro, Taima, Masuo, and Simidu, Sodi: The Effect of Ground on the Aerodynamic Characteristics of a Monoplane Wing. Rep. No. 156 (vol. XIII, 2), Aero. Res. Inst., Tokyo Imperial Univ., Sept. 1937.
7. Tani, Itiro, Itokawa, Hideo, and Taima, Masuo: Further Studies of the Ground Effect on the Aerodynamic Characteristics of an Aeroplane, with Special Reference to Tail Moment. Rep. No. 158 (vol. XIII, 4), Aero. Res. Inst., Tokyo Imperial Univ., Nov. 1937.
8. Wetmore, J. W., and Turner, L. I., Jr.: Determination of Ground Effect from Tests of a Glider in Towed Flight. Rep. No. 695, NACA, 1940.

U. S. GOVERNMENT PRINTING OFFICE: 1943

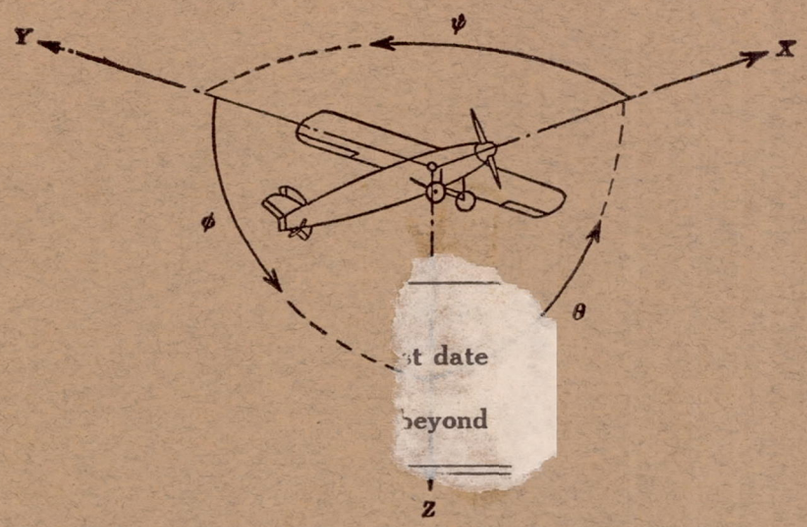

Positive directions of axes and angles (forces and moments) are shown by arrows

Axis		Force (parallel to axis) symbol	Moment about axis			Angle		Velocities	
Designation	Symbol		Designation	Symbol	Positive direction	Designation	Symbol	Linear (component along axis)	Angular
Longitudinal	X	X	Rolling	L	$Y \longrightarrow Z$	Roll	φ	u	p
Lateral	Y	Y	Pitching	M	$Z \longrightarrow X$	Pitch	θ	v	q
Normal	Z	Z	Yawing	N	$X \longrightarrow Y$	Yaw	ψ	w	r

Absolute coefficients of moment

$C_l = \frac{L}{qbS}$ (rolling) $\quad C_m = \frac{M}{qcS}$ (pitching) $\quad C_n = \frac{N}{qbS}$ (yawing)

Angle of set of control surface (relative to neutral position), δ. (Indicate surface by proper subscript.)

4. PROPELLER SYMBOLS

D Diameter

p Geometric pitch

p/D Pitch ratio

V' Inflow velocity

V_s Slipstream velocity

T Thrust, absolute coefficient $C_T = \frac{T}{\rho n^2 D^4}$

Q Torque, absolute coefficient $C_Q = \frac{Q}{\rho n^2 D^5}$

P Power, absolute coefficient $C_P = \frac{P}{\rho n^3 D^5}$

C_s Speed-power coefficient $= \sqrt[5]{\frac{\rho V^5}{P n^2}}$

η Efficiency

n Revolutions per second, rps

Φ Effective helix angle $= \tan^{-1}\left(\frac{V}{2\pi r n}\right)$

5. NUMERICAL RELATIONS

1 hp=76.04 kg-m/s=550 ft-lb/sec

1 metric horsepower=0.9863 hp

1 mph=0.4470 mps

1 mps=2.2369 mph

1 lb=0.4536 kg

1 kg=2.2046 lb

1 mi=1,609.35 m=5,280 ft

1 m=3.2808 ft